Resources, Conservation & Recycling 179 (2022) 106135

Contents lists available at ScienceDirect

Resources, Conservation & Recycling

journal homepage: www.elsevier.com/locate/resconrec

pH adjustment improves the removal of disinfection byproduct precursors from sedimentation sludge water

Yunkun Qian [a], Yanan Chen [a], David Hanigan [b], Yijun Shi [a], Sainan Sun [a], Yue Hu [a], Dong An [a,c,*]

[a] Department of Environmental Science & Engineering, Fudan University, Shanghai 200238, China
[b] Department of Civil and Environmental Engineering, University of Nevada, Reno, NV 89557-0258, United States
[c] Shanghai Institute of Pollution Control and Ecological Security, Shanghai 200092, China

ARTICLE INFO

Keywords:
Molecular composition
Disinfection byproducts
Sedimentation sludge water
Dissolved organic matter
FT-ICR-MS

ABSTRACT

Recycling sedimentation sludge water (SSW) supernatant to the head of drinking water treatment plants also recycles a large fraction of dissovled disinfection byproduct (DBP) precursors, contributing to the overall DBP load of the finished water. pH adjustment of SSW before release to settling ponds may result in incidental enhanced coagulation due to a significant amount of residual coagulant present in SSW, potentially removing DBP precursors. We adjusted the pH of SSW to 5, 6, 7, 8, and 9, and simulated recycling via mixing, sedimentation, and filtration. Samples settled at pH 5 or 6 formed the least DBPs, dependent on species, illustrating that buffering pH at slightly acidic conditions is an effective DBP precursor treatment strategy during SSW recycling. Carbonaceous DBP formation increased with increasing pH. An overall decrease in dissolved organic carbon at acidic conditions was observed, likely due to some enhanced coagulation and sedimentation of dissolved compounds. For nitrogenous DBPs (N-DBPs), samples at pH 5, 8, and 9 had greater formation than at pH 6 and 7. Fourier transform ion cyclotron resonance mass spectrometry revealed that adjusting pH to 8 and 9 increased the presence of highly unsaturated molecules, while the unsaturated nitrogen-containing formulae were removed at pH 6 and 7. N-DBP formation potential and the intensity (i.e., concentration) of CHON formulae with double bond equivalent > 10 were well correlated, demonstrating that alkaline pH SSW should be avoided to minimize formation/release of nitrogenous compounds and subsequent N-DBP formation.

1. Introduction

Water resources have become increasingly stressed due to environment pollution and global population growth. Recycling wastewater produced by drinking water treatment plants (DWTPs) improves water use efficiency and reduces the cost of treatment and transportation (Bourgeois et al., 2004; Li et al., 2018). Wastewater produced by DWTPs includes filter backwash water (FBW) and sedimentation sludge water (SSW), accounting for approximately 2–10% of total DWTP intake flows (Curko et al., 2013; Walsh et al., 2008). Compared to FBW and typical influent waters, SSW contains significantly more suspended solids (i.e., particulate), natural organic matter (NOM) represented by dissolved organic carbon (DOC), and disinfection byproduct (DBP) precursors (Chen et al., 2015; Mccormick et al., 2010). Our recent research demonstrated that DOC and dissolved organic nitrogen (DON) concentrations in SSW were 2.1 and 1.8 times that of in FBW, respectively, and DBP formation potential (FP) concentration were 1.1–2.2 times FBW DBP FPs (Hu et al., 2021; Qian et al., 2020). The summative calculated toxicity of measured DBPs in SSW was also higher than that in FBW after chlorination. Therefore, SSW is likely the most challenging to treat and reuse, but if successful, provides an opportunity for resource recovery.

In China, SSW is usually discharged to surface water after treated by thickener-induced precipitation, which removes suspended solids well but has little impact on dissolved organic matter (DOM), and DOM impacts receiving ecosystems by depleting dissolved oxygen. Another treatment method is to pump SSW to intermittent storage tanks or settling ponds, which settle much of the suspended solids, and the supernatant is then recycled to the head of the DWTP and blended with incoming raw water. Again, this poorly removes DOM and previous studies have shown that the formation of some specific DBP classes (e.g., nitrosamines, trihalomethanes (THMs), and haloacetic acids (HAAs)) increased when recycling SSW supernatant. The recycled DOM contributed 8–31% of the finished water DBP loading (Walsh et al., 2008; Westerhoff et al., 2019). Therefore, SSW treatment to remove

* Corresponding author.
E-mail address: andong@fudan.edu.cn (D. An).

https://doi.org/10.1016/j.resconrec.2021.106135
Received 17 August 2021; Received in revised form 6 December 2021; Accepted 27 December 2021
Available online 3 January 2022

DOM, DBPs, and DBP precursors before recycling will positively impact finished water quality and water use efficiency.

Coagulation and sedimentation remove suspended solids well from water (Bachand et al., 2019; Lin et al., 2018; Liu et al., 2016). But traditional coagulation and sedimentation poorly remove DOM and DBP precursors. Researchers have attempted to improve removal of DOM and DBP precursors by enhanced coagulation, and obtained excellent removal (Guo et al., 2017; Ulu et al., 2019; Zhao et al., 2013). However, treatment of SSW by either traditional or enhanced coagulation requires additional on-site infrastructure, increasing the cost and complexity of treatment. pH adjustment of SSW before storage in tanks or settling ponds may mimic enhanced coagulation because there is a significant amount of residual coagulant present (Cao et al., 2011). Thus, pH adjustment of SSW may be a relatively simple method to enhance finished water quality and reduce water waste.

DBP precursors are generally low molecular weight compounds, including the precursors for the highly toxic DBPs haloacetonitriles (HANs) and haloacetamides (HAMs) (An et al., 2019; Qian et al., 2020). One challenge with pH adjustment of SSW may be that the higher molecular weight organic matter may be altered/hydrolyzed, which may form new precursor material and influence the formation of DBPs (Baker et al., 2007; Meng et al., 2017; Zhang et al., 2009).

To investigate the potential treatment of SSW via pH adjustment, we collected SSW samples from a traditional DWTP and adjusted the pH to between 5 and 9. Samples were mixed, settled, and filtered to represent downstream DWTP processes. Four THMs, nine HAAs, seven HANs, six HAMs, and the change in DOM composition via mass spectrometry were measured. The objective was to investigate changes to DOM composition and DBP formation. We draw conclusions based on the correlations between DBP FP and Fourier transform ion cyclotron resonance mass spectrometry (FT-ICR-MS) formulae and signal intensity.

2. Materials and methods

2.1. Chemical reagents

Standards of four THMs, nine HAAs, seven HANs, and six HAMs in methyl *tert*-butyl ether (MTBE) were purchased from Dr. Ehrenstorfer (Augsburg, Germany). Detailed information on DBPs is described in Supplemental Information. Methyl *tert*-butyl ether (high performance liquid chromatography grade) was purchased from Sigma Aldrich (St. Louis, MO, USA). Ultrapure water with a resistivity of 18.2 MΩ•cm was prepared using a Gradient A10 ultrapure water system (Milli-Q®, Millipore Corporation, Bedford, MA, USA). Sodium hypochlorite (NaClO, analytical grade, 99%) and other reagents (analytical grade) were obtained from the Sinopharm Chemical Reagent Co., Ltd. (Shanghai, China).

2.2. Sedimentation sludge sample collection and treatment

Sedimentation sludge samples were collected from a conventional drinking water treatment plant in Shanghai, China which treats Yangtze River water with coagulation, sedimentation, filtration, and disinfection. The samples of sludge were collected in amber glass bottles from the outlet of the sludge discharge pipe from the sedimentation tank and stored at 4 °C in refrigerators until use. Aluminum sulfate was used as coagulant during coagulation at the drinking water treatment plant in the pH range of 6.5–7.5. pH of raw water and SSW was 8.2 ± 0.1 and 7.43 ± 0.1, respectively.

The pH of SSW was adjusted to 5, 6, 7, 8, and 9 using 1 mol/L hydrochloric acid solution and 1 mol/L sodium hydroxide solution, respectively. Samples were then mixed with a Jar tester (ZR4–6, Zhongrun water industry technology development CO., LTD.) at 150 rpm for 60 min at room temperature, similar to mixing provided in sludge buffer tanks in China. After 30 min of sedimentation the supernatants were filtered with 0.45 μm glass fiber filters. The pH of all the samples was adjusted to 7 after filtration before further experimentation and/or analysis to allow for comparison of DBP FPs. The raw sample (not pH adjusted) was mixed, settled, and filtered the same as the control experiment, and is further referred to as the untreated sample. Water quality characteristics of the SSW are listed in Table S2. An example image of samples before and after treatment is shown in Figure S1.

2.3. MW fractionation

A Minimate™ II tangential flow filtration (TFF) system (Pall Corporation, USA) with Ultracel®-PL ultrafiltration membranes (Millipore Sigma, USA) was used to fractionate water samples into nominal MW fractions of < 3, < 10, and < 100 kDa fractions (Figure S2). The concentration of DOC in the filtrates was determined directly and expressed as fractions of total DOC by subtraction of lower MW filtrate DOC concentrations (e.g., concentration in the 3 – 10 kDa fraction was equal to that measured in the < 10 kDa filtrate minus the concentration in the < 3 kDa filtrate). Further methodology is provided in our previous publications (An et al., 2017; Qian et al., 2020) and in the Supplemental Information.

2.4. FT-ICR-MS analysis

100 mL of each treated water sample was solid-phase extracted using Bond Elut PPL cartridges (500 mg, 6 mL, Agilent Technologies, USA). Cartridges were first conditioned with methanol (HPLC grade, 20 mL) and acidified ultrapure water (pH = 2, 20 mL). Water samples were acidified with hydrochloric acid to pH 2 and passed through PPL cartridges by gravity at approximately 2 mL/min. Cartridges were rinsed with 20 mL of acidified ultrapure water to remove salt and dried by passing ultrapure N_2 gas. Organic matter was eluted with 6 mL of methanol and stored at −18 °C in the dark until FT-ICR-MS analysis. An ultrapure water sample was also extracted using a PPL cartridge and then eluted in order to serve as procedural blank in the FT-ICR-MS analysis.

FT-ICR-MS (SolariX 7.0T, Bruker, USA) in ESI- mode was used to analyze the molecular composition of organic matter. Initial experiments in ESI+ resulted in a significant number of sodium adducts which made formulae assignment challenging and thus only ESI- results are presented. Briefly, samples were injected into the source at 180 μL/h by a syringe pump. The spray shield voltage, capillary voltage, and cone voltage were 4.0 kV, 4.5 kV, and −320 V, respectively. Ionized substances were accumulated in a hexapole trap and an argon filled hexapole collision cell for 0.1 and 1 s, respectively, before being directed to the ICR detector. The mass range was set at m/z 100−1000. Notably, the FT-ICR-MS mass range is entirely contained within the <3 kDa fraction and conclusions made from the MS measurements are therefore only reflective of this fraction. Each spectrum was scanned 128 times.

HPLC grade methanol and extracted ultrapure water samples were measured as solvent and procedural blanks. Peaks found in blanks were removed from the lists of peaks in samples. Molecular formulae were determined by Bruker DataAnalysis software (version 4.0) and Matlab routines (Fu et al., 2020). Only mass peaks with signal to noise (S/N) ratios > 10 were considered. Molecular formulae were limited to the following elemental combinations: $^{12}C_{1-100}$, $^{1}H_{1-100}$, $^{16}O_{0-50}$, $^{14}N_{0-5}$, $^{13}C_{0-1}$, $^{32}S_{0-3}$, $^{31}P_{0-2}$, and mass error between the assigned formula and the measured mass was limited to a maximum of 1 ppm. DOM molecular formulae were delineated into seven categories by elemental ratios (O/C and H/C) (Fu et al., 2020; Li et al., 2018; Feng et al., 2016): (1) lipids and proteins (O/C = 0 − 0.52, H/C = 1.5 − 2.2), (2) amino sugars (O/C = 0.52−0.71, H/C = 1.5 − 2.2), (3) carbohydrates (O/C = 0.71−1.2, H/C = 1.5 − 2.4), (4) unsaturated hydrocarbons (O/C = 0 − 0.1, H/C = 0.7 − 1.5), (5) lignins (O/C = 0.1 − 0.67, H/C = 0.7 − 1.5), (6) tannins (O/C = 0.67−1.2, H/C = 0.5 − 1.5), and (7) condensed hydrocarbons (O/C = 0 − 0.67, H/C = 0.2 − 0.7).

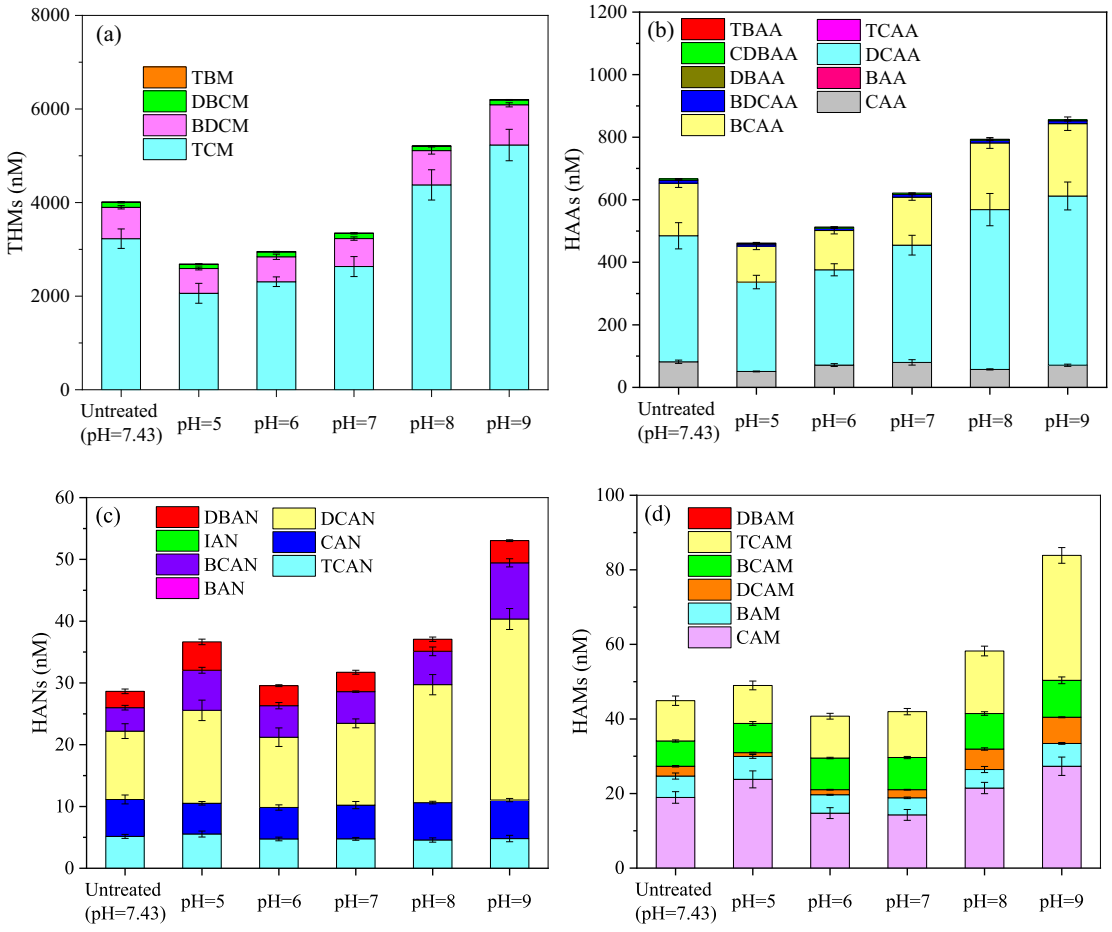

Fig. 1. (a) THM, (b) HAA, (c) HAN, and (d) HAM formation in the samples coagulated at varying pH and filtered with a 0.45 μm nominal pore size filter. The untreated sample was mixed, settled, filtered and had a pH = 7.43. Error bars represent one standard deviation (n = 3).

2.5. Additional analytical methods

DOC was measured by a total organic carbon (TOC) analyzer (Multi N/C 2100, Analytik Jena AG, Germany). UV_{254} was measured using a spectrophotometer (DR6000, HACH, USA). DBP formation potential (FP) tests have been described in detail in previous literature (Qian et al., 2020) and in the Supplemental Information. Four THMs, nine HAAs, seven HANs, and six HAMs were analyzed by liquid-liquid extraction (LLE) and gas chromatography (GC, 7890B, Agilent Technologies, USA) equipped with an electron capture detector (ECD, Agilent Technologies, USA). Detailed information on the analytical methods for DBPs are described in previously published procedures (An et al., 2013; Qian et al., 2020) and Supplemental Information. All experiments were conducted in triplicate.

3. Results and discussion

3.1. DBP FP after pH treatment

Trichloromethane (TCM), dichloroacetic acid (DCAA), dichloroacetonitrile (DCAN), and 2-chloroacetamide (CAM) were the primary species of THMs, HAAs, HANs, and HAMs, and accounted for 34–84% of the total THM, HAA, HAN, and HAM formations, respectively (Fig. 1), consistent with the results from our previous research conducted on SSW (Qian et al., 2021). The formation of carbonaceous DBPs (C-DBPs) increased as the pH increased from 5 to 9 and all samples at alkaline pH had greater C-DBP formation than the untreated sample (pH = 7.43, mixed, settled, filtered without pH adjustment). Compared to the untreated sample, acidic and neutral samples had lower concentrations of C-DBP precursors, likely due to enhanced coagulation and sedimentation of sludge. Therefore, adding acid, settling, and filtering was effective at controlling the formation of C-DBPs in SSW during disinfection process, but more alkaline conditions tended to release new precursors or transform some precursors to more reactive material.

The formation of nitrogenous DBPs (N-DBPs) increased with increasing pH from 6 to 9. The sample treated at pH 5 did not follow the trend and had greater N-DBP FP than the untreated sample, approximately equivalent to the sample treated at pH 8. N-DBP yield on a carbon basis was also elevated. Thus, it is likely that at both pH 5 and alkaline pH, N-DBPs precursors were released by hydrolysis of larger organic compounds and the lower molecular weight hydrolysis products were not removed by filtration. The different behavior of C- and N-DBP precursors at reduced pH suggests that the groups of precursors are distinctly different, having different reactivity after acidic treatment. In general, slightly acidic (pH 6) conditions balanced C- and N-DBPs and resulted in the lowest total DBP formation. However, at lower pH (pH 5), there was an increase in N-DBP FP, which is concerning because N-DBPs are generally orders of magnitude more toxic than C-DBPs (Wagner and Plewa, 2017).

3.2. MW distribution effects on DBP FP

Mixing, settling, and filtering at acidic pH resulted in DOC concentrations slightly less than that of the untreated sample; 3.17 mg/L and 3.35 mg/L at pH 5 and 6, respectively, compared to 3.65 mg/L in the untreated sample (Table S1). But at pH 8 and 9, DOC concentrations increased significantly, 8.67 mg/L and 9.45 mg/L, respectively. Thus, acidic pH likely caused some limited coagulation and sedimentation of

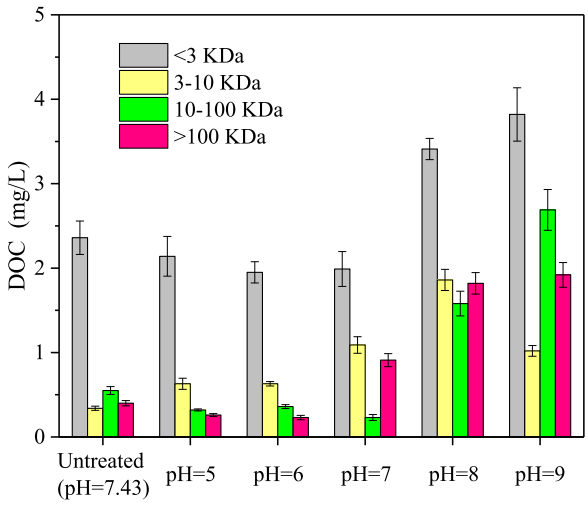

Fig. 2. DOC concentration in different MW fractions of samples coagulated at varying pH and filtered with a 0.45 μm nominal pore size filter. Error bars represent one standard deviation of experimental replicates (n = 3).

dissolved compounds, which is well reflected in the reduced formation of DBPs. At alkaline pH, organic compounds were released from larger settleable/filterable solids which would have otherwise been removed by filtration.

Fig. 2 shows the MW distribution of DOM in pH adjusted and untreated samples. Low MW organic matter is generally thought to dominate the DBP precursor pool (Hua and Reckhow, 2007; Qian et al., 2020; Zhang et al., 2018) and both conventional and advanced treatment processes remove low MW organic matter poorly (Han et al., 2015; Hanigan et al., 2015). DOC in the < 3 kDa fraction accounted for > 39% of the total DOC across all treatments, greater than all other fractions for all samples. The MW distribution among the untreated, neutral and acidic samples was similar, although the concentration of < 3 kDa organic matter in acidic samples was slightly less than that in untreated samples, and the 3–10 kDa fraction slightly greater, reflective of agglomeration of low MW neutrals into higher mass compounds, or agglomeration of colloidal and suspended particulates followed by sorption of lower MW compounds. Our previous studies indicated that low MW (< 3 kDa) organic matters were the primary precursors of DBP, including THMs, HAAs, HAN, and HAMs in SSW (Hu et al., 2021; Qian et al., 2020). Therefore, such a reduction in the lower MW DOC is likely responsible for the reduced DBP formation.

At neutral and alkaline pH, the proportion of < 3 kDa fraction decreased to 40%–47% of the total DOC, and the proportion of high MW (> 10 kDa) organic material increased to 27%–49%. Although the fractional contribution to DOC decreased for the <3 kDa fraction, the overall DOC in this fraction (and in the bulk sample) increased significantly, likely due to the hydrolysis of the flocs or increasing solubility or larger molecules at alkaline pH. This resulted in greater overall DBP FP, although the yield of DBPs on a carbon basis was reduced (Figure S4). Thus, slightly acidic pH was the most beneficial for removal of both DBP precursors and organic matter.

3.3. Effects of molecular composition on DBP FP

3.3.1. Molecular weight and saturation

To further understand the mechanisms impacting increased or decreased DBP formation after SSW treatment at varying pH, we conducted FT-ICR-MS of the residual organic matter. The MW and double bond equivalent (DBE) distributions are displayed as kernel-based cumulative density plots (violin plots) in Fig. 3 (raw mass spectra shown in Figure S3). Table 1 contains the intensity weighted average elemental compositions. The neutral mass (m/z plus mass of a proton, assuming singly charged and deprotonated ions) of > 83% of the molecular formulae occurred in the range of 200–600 Da for nearly all samples. However, for the water sample treated at pH 9, the molecular formulae of compounds with mass between 600 and 1000 Da accounted for more than 47% of the total molecular formulae. The intensity weighted average neutral mass was 562 Da for the water sample treated at pH 9, compared to ~425 Da for all other samples. Notably the instrument was set to scan from 100 to 1000 m/z, which does not capture the full range of the masses captured in the fractionation experiments. But, organic matter in the higher MW fractions measured by mass spectrometry (600–1000 Da) corresponds to the low MW fraction from fractionation

Table 1
Intensity weighted average elemental compositions of DOM identified by FT-ICR-MS.

Water sample	Number of assigned formulae	MW_{wa} (Da)	O/C_{wa}	H/C_{wa}	N/C_{wa}	DBE_{wa}	DBE/C_{wa}
Untreated	2566	428.80	0.37	1.46	0.03	7.02	0.37
pH=5	3602	449.24	0.39	1.40	0.03	8.13	0.39
pH=6	2805	437.03	0.36	1.46	0.03	7.44	0.35
pH=7	2718	457.15	0.36	1.45	0.03	7.92	0.35
pH=8	2885	437.57	0.44	1.28	0.08	8.40	0.48
pH=9	2677	561.53	0.36	1.50	0.05	8.36	0.34

wa = intensity weighted average.

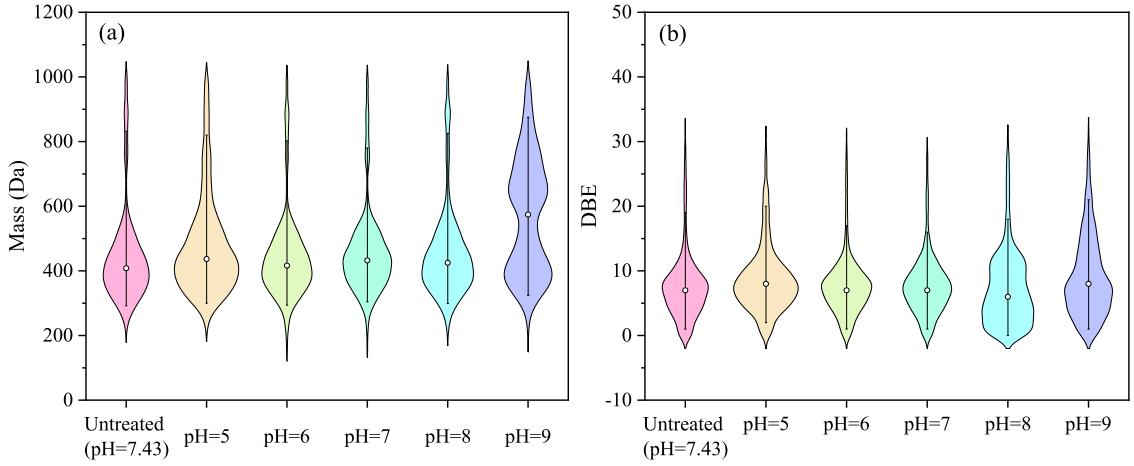

Fig. 3. Kernel-based cumulative density plots (violin plots) displaying the intensity weighted distribution of (a) molecular mass and (b) DBE for assigned formulas. White dots indicate median values, whiskers indicate upper and lower quartiles.

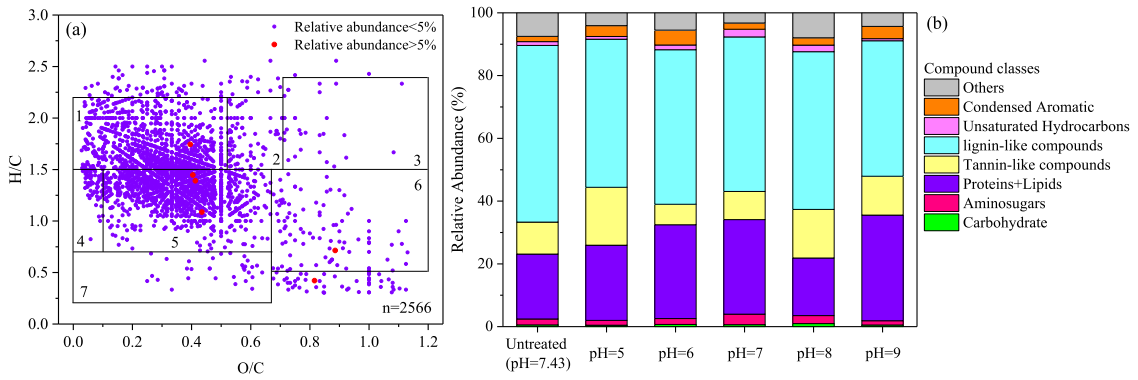

Fig. 4. (a) Example Van Krevelen plot (untreated sample, pH = 7.43), and (b) intensity weighted relative abundance of DOM composition. Rectangles indicate regions associated with (1) lipids and proteins, (2) amino sugars, (3) carbohydrates, (4) unsaturated hydrocarbons, (5) lignins, (6) tannins, and (7) condensed hydrocarbons. Relative abundance is calculated as ion current of a single *m/z* divided by the total ion current of all *m/z* with assigned formulae.

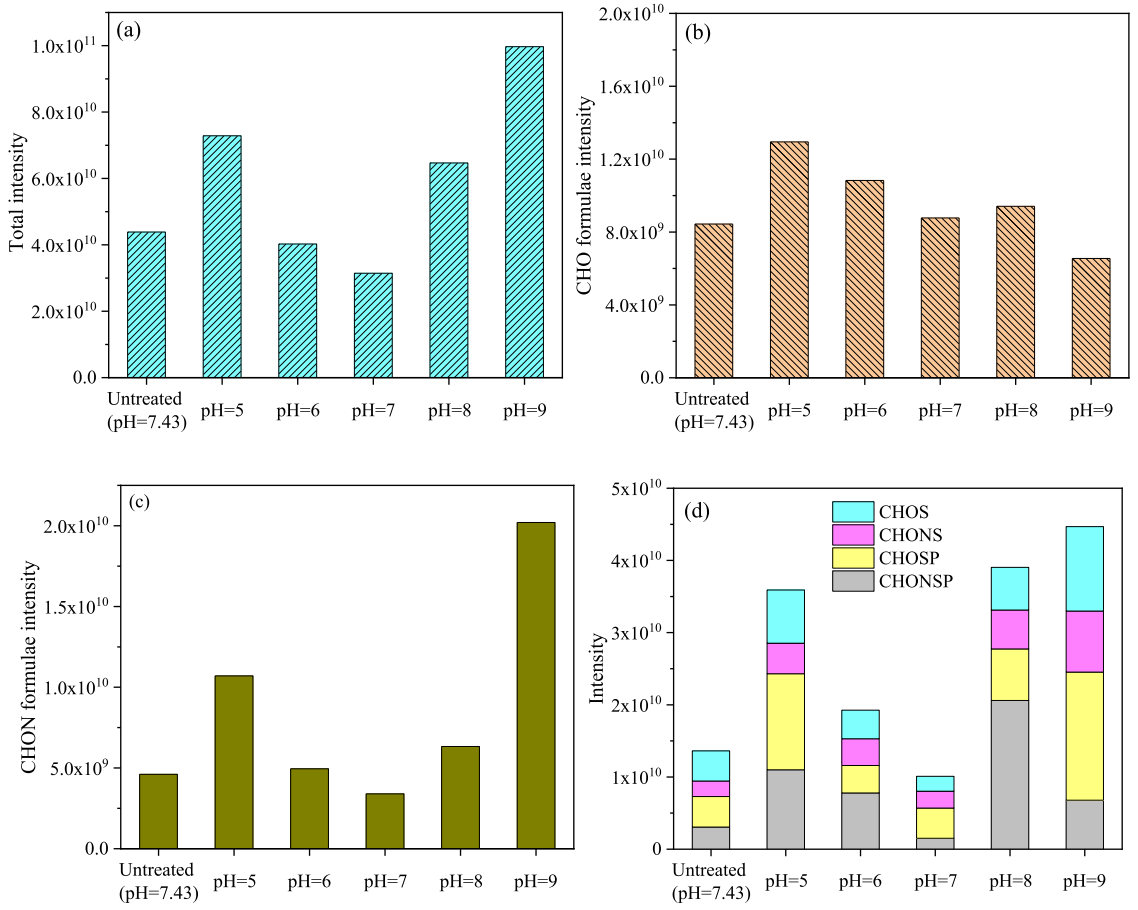

Fig. 5. Cumulative intensity of (a) all ions, (b) only CHO formulae, (c) only CHON formulae, and (d) only sulfur containing formulae.

experiments. Thus, when comparing the fractionation experiments to these experiments, there is agreement that at pH 9 some additional organic matter was released and was not removed by settling or filtration, and it is apparent that the released organic matter is slightly greater mass than that which is present in lower pH samples. These compounds likely account for the increase in C-DBP FP at increased pH.

Previous studies have shown that highly unsaturated NOM molecules are more reactive toward chlorine than those that are more saturated, and chloroform FP has been shown to be correlated with increasing degree of unsaturation (Lavonen et al., 2013; Wang et al., 2017; Zhang et al., 2012a). DBE was used to evaluate the degree of saturation (Stubbins et al., 2010; Zhang et al., 2019). The intensity weighted average DBEs (DBE_{wa}) were 8.36 and 8.40 at pH 8 and 9, respectively, higher than that at acidic and neutral pH (7.02 – 8.13). Therefore, the organic matter released from filterable sludge flocs at alkaline pH was less saturated than that in acid and neutral pH, further contributing to increased C-DBP FP.

Figs. 4 and S5 are Van Krevelen plots of all compounds measured and reveal that lignin-like compounds were the dominant components of DOM in all water samples, accounting for 43%–56% of all compounds. This is consistent with previous studies that conclude that DOM in environmental water samples contains a large fraction of lignin-like compounds, typically composed of aromatic polymeric structures, such as syringyl and p-hydroxyphenylpropane moieties (Nebbioso and

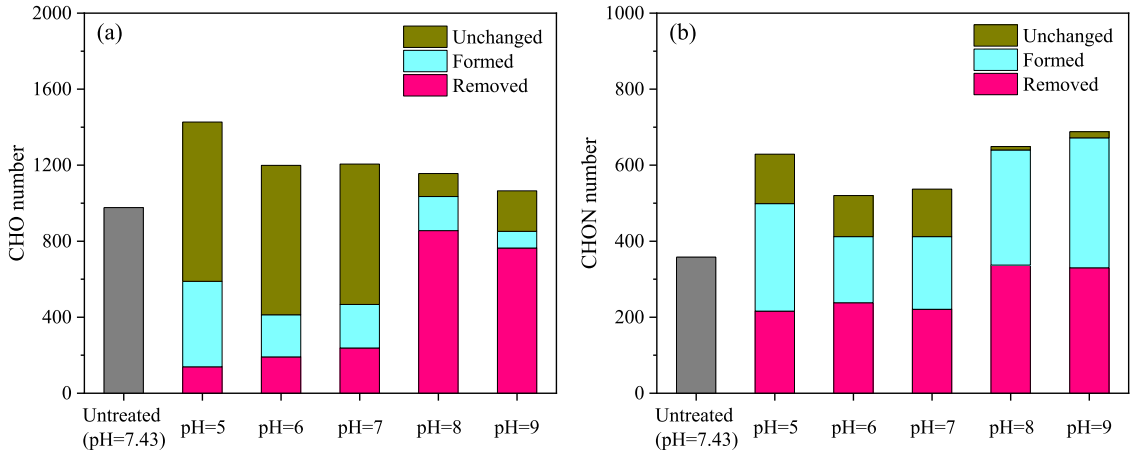

Fig. 6. Number of (a) CHO and (b) CHON formulae unchanged (present in both the untreated and treated samples), formed (present in the treated sample but not the untreated sample) and removed (present in the untreated sample but not in the treated sample) after treatment at varying pH.

Piccolo, 2013; Phatthalung et al., 2021; Zhang et al., 2012b). These lignin-like compounds are likely to be refractory and have been shown to be an important source of DBPs (e.g., HAAs, HANs, HAMs and haloacetaldehydes) during chlor(am)ination (Chuang et al., 2015; Hua et al., 2014; Sanchís et al., 2020). Water samples treated at pH 5, 8, and 9 had a higher intensity of lignin-like compounds than other water samples (Figure S6), and treatment at this pH also resulted in the greatest formation of N- and C-DBPs.

3.3.2. *CHO/CHON formulae*

CHO and CHON formulae are classes of molecular formulae most closely related to the formation of C-DBPs and N-DBPs during chlorination, respectively (Zhang et al., 2019). As for CHO containing compounds, the total number of formulae (i.e., diversity of dissolved compounds) and cumulative intensity of all CHO formulae (i.e., concentration) decreased as the pH increased from 5 to 9 (Table S3 and Fig. 5b). The weighted average H/C of CHO formulae at alkaline pH was lower than at other pH, and, correspondingly, the weighted average O/C was higher (Table S3), consistent with the findings from DBE, where unsaturation tended to increase with pH. The finding that the number of and intensity of CHO compounds decreased with increasing pH is somewhat contradictory to the C-DBP findings, but it could be that the

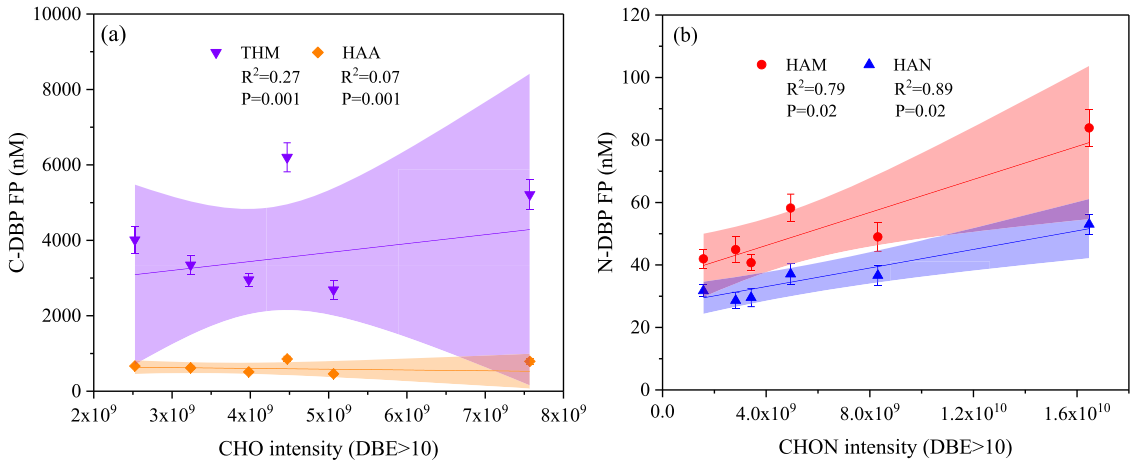

Fig. 7. Correlation between DBP FP in all samples (untreated, pH 5, 6, 7, 8 and 9) and cumulative ion intensity of relatively unsaturated compounds (DBE > 10). Error bars represent one standard deviation of experimental replicates (n = 3).

additional released DOM (pH 8 and 9) had higher ionization efficiency with the consequence that the other CHO (apparently lost) could not further be detected. Another possibility is that compounds which contain CHO only do not perfectly represent the pool of C-DBP precursors.

In Figs. 5d and S7 it can be seen that CHOS, CHONS, CHOSP, CHONSP compounds were formed at alkaline pH. Thus, it is possible that heteroatom (e.g., N, S, and P) addition reactions with CHO compounds were the primary mechanism for the removal of CHO formulae at alkaline pH (Feng et al., 2015; Jackson et al., 2017; Qian et al., 2011). Another possibility is base catalyzed condensation reactions of CHO and CHONP/CHONS/CHOSP/CHONSP. Previous studies had shown that sulfur and nitrogen containing organic matter are reactive N-DBP precursors (Ding et al., 2019; Yang et al., 2012), potentially explaining higher levels of N-DBP formation at pH 8 and 9, but not at pH 5.

The total number of CHON compounds (Table S3), formation of new CHON compounds (Fig. 6b), and cumulative intensity of CHON formulae (Fig. 5c) increased at pH 5 and 9, and decreased at pH 6 or 7. More than 96% of the initial CHON formulae were removed to below the instrument detection limit and more than 88% of the CHON formulae at pH 8 and 9 were newly formed as a consequence of pH treatment (Fig. 6b). CHON formulae also had higher H/C_{wa} and lower DBE_{wa} values at pH 6 and 7 than that at other pH (Table S4). Together, these results illustrate that unsaturated nitrogen-containing DOM was removed at pH 6 and 7, attributable for the decrease of N-DBP FP.

3.3.3. *Relationship between DBP FP and CHO/CHON*

To determine the most important precursor material in the treated samples we attempted to discover correlations between assigned formulae and DBP formation. The number and intensity of CHO formulae decreased with increasing pH (Table S3 and Fig. 5) but C-DBP concentrations increased. Thus, it is no surprise that there was no significant correlation (R^2 = 0.07–0.43, $P < 0.01$) between C-DBP FP and the cumulative intensity of all CHO compounds (Figure S8a), or CHO compounds with DBE > 10 (Fig. 7a). This suggests that low MW (< 1 kDa) organic matter with only CHO in the structure were not the primary precursors of C-DBPs, or the primary precursor pool may be in organic matter greater than the instrumental scan range (100–1000 m/z).

N-DBPs were also poorly correlated with the total number of CHON compounds and CHON cumulative ion intensity (Figure S8b), but there was a significant positive correlation (R^2 = 0.79–0.89, $P < 0.05$) between N-DBP formation and the cumulative intensity of all CHON formulae with DBE > 10 (Fig. 7b). Thus, the primary precursor pool for HANs and HAMs was relatively unsaturated CHON containing compounds. Further research should confirm these conclusions in other SSWs and other drinking water sources. Attempts to reduce N-DBP formation in SSW and, likely drinking water as a whole should focus on removal of relatively unsaturated organic N.

4. Conlusions

Recycling SSW improves water use efficiency but contributes the formation of C- and N-DBPs during drinking water treatment and the contents and characteristics of NOM affect the formation of DBPs. pH adjustment before simluated sludge storage had two effects on the sludge, 1) in some cases NOM was removed, likely though coagulation and sedimentation, reducing formation of C-DBPs to a significant extent, and reducing the formation of N-DBPs to a lesser extent, and 2) the overall characteristics of the remaining NOM were changed significantly, in some cases resulting in greater reactivity towards N-DBPs. For example, pH adjustment to 5 effectively minimized the formation of C-DBPs, and pH 6 minimized the formation of N-DBPs during SSW recycling. Reducing the pH to 6 prior to storage, approximately 1.5 units from the raw SSW, would effectively balance the reduction in N- and C-DBPs. The ion intensity of compounds containing CHON, CHOS, CHONS, CHOSP, and CHONSP and the concentration of DBP FP in the samples treated at pH 6 and 7 were lower than that in other samples. But at alkaline pH, SSW contained more highly unsaturated organic matter, which although less reactive in terms of yield, still resulted in greater formation of C- and N-DBPs. No correlation was observable between various organic matter characteristics and C-DBP FP, but relatively unsaturated CHON formulae were significantly correlated with the formation of N-DBPs. Other more effective removal strategies for relatively unsaturated CHON formulae should be further employed to minimize the formation of N-DBPs and ensure the safety of finished water during SSW recycling.

Credit author statement

Yunkun Qian: Conceptualization, Methodology, Investigation, Writing - Original draft preparation, Visualization
Yanan Chen: Validation, Data curation
David Hanigan:Writing - Review and Editing
Yijun Shi:Validation, Data curation
Sainan Sun:Formal analysis
Yue Hu:Investigation
Dong An:Conceptualization, Resources, Supervision, Project administration, Funding acquisition

Declaration of Competing Interest

The authors declare that they have no known competing financial interests or personal relationships that could have appeared to influence the work reported in this paper.

Acknowledgements

This research is supported by the National Natural Science Foundation of China (NSFC 22076026, 21777031, 21577024) and partially by the National Science Foundation (CBET-1804255).

Supplementary materials

Supplementary material associated with this article can be found, in the online version, at doi:10.1016/j.resconrec.2021.106135.

References

An, D., Chen, Y., Gu, B., Westerhoff, P., Hanigan, D., Herckes, P., Fischer, N., Donovan, S., Croue, J.P., Atkinson, A., 2019. Lower molecular weight fractions of PolyDADMAC coagulants disproportionately contribute to N-nitrosodimethylamine formation during water treatment. Water Res 150, 466–472.

An, D., Chen, M., Shen, Y., 2013. Analyses of molecular weight distribution of organic matters with pre-oxidation and PAC-UF pretreatment before seawater reverse osmosis. Desalin. Water Treat. 51 (19), 3920–3924.

An, D., Gu, B., Sun, S., Zhang, H., Chen, Y., Zhu, H., Shi, J., Tong, J., 2017. Relationship between THMs/NDMA formation potential and molecular weight of organic compounds for source and treated water in Shanghai, China. Sci. Total Environ. 605–606, 1–8.

Bachand, S.M., Kraus, T.E.C., Stern, D., Liang, Y., Bachand, P.A.M., 2019. Aluminum- and iron-based coagulation for in-situ removal of dissolved organic carbon, disinfection byproducts, mercury and other constituents from agricultural drain water. Ecol. Eng. 134, 26–38.

Baker, A., Elliott, S., Lead, J.R.J.C., 2007. Effects of filtration and pH perturbation on freshwater organic matter fluorescence. Chemosphere 67 (10), 2035–2043.

Bourgeois, J.C., Walsh, M.E., Gagnon, G.A., 2004. Comparison of process options for treatment of water treatment residual streams. J. Environ. Eng. Sci. 3 (6), 477–484.

Cao, B., Gao, B., Liu, X., Wang, M., Yang, Z., Yue, Q., 2011. The impact of pH on floc structure characteristic of polyferric chloride in a low DOC and high alkalinity surface water treatment. Water Res 45 (18), 6181–6188.

Chen, T., Xu, Y., Zhu, S., Cui, F., 2015. Combining physico-chemical analysis with a Daphnia magna bioassay to evaluate a recycling technology for drinking water treatment plant waste residuals. Ecotox. Environ. Safe. 122, 368–376.

Chuang, Y.H., Mccurry, D.L., Tung, H.H., Mitch, W.A., 2015. Formation pathways and trade-offs between haloacetamides and haloacetaldehydes during combined chlorination and chloramination of Lignin Phenols and natural waters. Environ. Sci. Technol. 49 (24), 14432–14440.

Curko, J., Mijatovic, I., Rumora, D., Crnek, V., Matosic, M., Nezic, M., 2013. Treatment of spent filter backwash water from drinking water treatment with immersed ultrafiltration membranes. Desalin Water Treat 51 (25–27), 4901–4906.

Ding, S., Wang, F., Chu, W., Fang, C., Du, E., Yin, D., Gao, N., 2019. Effect of reduced sulfur group on the formation of CX3R-type disinfection by-products during chlor (am)ination of reduced sulfur compounds. Chem. Eng. J 361, 227–234.

Feng, L., Xu, J., Kang, S., Li, X., Li, Y., Jiang, B., Shi, Q., 2016. Chemical composition of microbe-derived dissolved organic matter in cryoconite in Tibetan Plateau glaciers: insights from Fourier transform ion cyclotron resonance mass spectrometry analysis. Environ. Sci. Technol. 50 (24), 13215–13223.

Feng, L., Zhao, S., Sun, S., Wang, W., Gao, B., Yue, Q., 2015. Effect of pH with different purified aluminum species on coagulation performance and membrane fouling in coagulation/ultrafiltration process. J. Hazard. Mater. 300, 67–74.

Fu, Q., Fujii, M., Riedel, T., 2020. Development and comparison of formula assignment algorithms for ultrahigh-resolution mass spectra of natural organic matter. Anal. Chim. Acta 1125, 247–257.

Guo, T., Yang, Y., Liu, R., Li, X., 2017. Enhanced removal of intracellular organic matters (IOM) from Microcystic aeruginosa by aluminum coagulation. Sep. Purif. Technol. 189, 279–287.

Han, Q., Yan, H., Zhang, F., Xue, N., Wang, Y., Chu, Y., Gao, B., 2015. Trihalomethanes (THMs) precursor fractions removal by coagulation and adsorption for bio-treated municipal wastewater: molecular weight, hydrophobicity/hydrophily and fluorescence. J. Hazard. Mater. 297, 119–126.

Hanigan, D., Zhang, J., Herckes, P., Zhu, E., Krasner, S.W., Westerhoff, P., 2015. Contribution and removal of watershed and cationic polymer N-nitrosodimethylamine precursors. J. Am. Water Works Ass. 107 (3), 152–163.

Hu, Y., Qian, Y., Chen, Y., Guo, J., Song, J., An, D., 2021. Characteristics of trihalomethane and haloacetic acid precursors in filter backwash and sedimentation sludge waters during drinking water treatment. Sci. Total Environ. 775, 145952.

Hua, G., Kim, J., Reckhow, D.A., 2014. Disinfection byproduct formation from lignin precursors. Water Res 63, 285–295.

Hua, G., Reckhow, D.A., 2007. Characterization of disinfection byproduct precursors based on hydrophobicity and molecular size. Environ. Sci. Technol. 41 (9), 3309–3315.

Jackson, P.A., Widen, J.C., Harki, D.A., Brummond, K.M., 2017. Covalent modifiers: a chemical perspective on the reactivity of α,β-unsaturated carbonyls with thiols via Hetero-Michael addition reactions. J. Med. Chem. 60 (3), 839–885.

Lavonen, E.E., Gonsior, M., Tranvik, L.J., Schmitt-Kopplin, P., Kohler, S.J., 2013. Selective chlorination of natural organic matter: identification of previously unknown disinfection byproducts. Environ. Sci. Technol. 47 (5), 2264–2271.

Li, L., Xu, G., Xing, J., 2018. Diatomite enhanced dynamic membrane technology for simultaneous backwash sludge pre-dewatering and backwash wastewater recycling. J. Clean. Prod. 211, 1420–1426.

Lin, J., Hua, L., Hung, S., Huang, C., 2018. Algal removal from cyanobacteria-rich waters by preoxidation-assisted coagulation–flotation: effect of algogenic organic matter release on algal removal and trihalomethane formation. J. Environ. Sci. (China) 63 (001), 147–155.

Liu, Y., Duan, J., Li, W., Beecham, S., Mulcahy, D., 2016. Effects of organic matter removal from a wastewater secondary effluent by aluminum sulfate coagulation on haloacetic acids formation. Environ. Eng. Sci 33 (7), 484–493.

Mccormick, N.J., Porter, M., Walsh, M.E., 2010. Disinfection by-products in filter backwash water: implications to water quality in recycle designs. Water Res 44 (15), 4581–4589.

Meng, Y., Wang, M., Guo, B., Zhu, F., Wang, Y., Lu, J., Ma, D., Sun, Y., Gao, B., 2017. Characterization and C-, N-disinfection byproduct formation of dissolved organic matter in MBR and anaerobic-anoxic-oxic (AAO) processes. Chem. Eng. J 315, 243–250.

Nebbioso, A., Piccolo, A., 2013. Molecular characterization of dissolved organic matter (DOM): a critical review. Anal. Bioanal. Chem. 405, 109–124.

Phatthalung, W.N., Suttinun, O., Phungsai, P., Kasuga, I., Musikavong, C., 2021. Non-target screening of dissolved organic matter in raw water, coagulated water, and chlorinated water by Orbitrap mass spectrometry. Chemosphere 264 (2), 128437.

Qian, Y., Chen, Y., Hu, Y., Hanigan, D., Westerhoff, P., An, D., 2021. Formation and control of C- and N-DBPs during disinfection of filter backwash and sedimentation sludge water in drinking water treatment. Water Res 18, 116964.

Qian, Y., Hu, Y., Chen, Y., An, D., Westerhoff, P., Hanigan, D., Chu, W., 2020. Haloacetonitriles and haloacetamides precursors in filter backwash and sedimentation sludge water during drinking water treatment. Water Res 186, 116346.

Qian, Y., Karpus, J., Kabil, O., Zhang, S., Zhu, H., Banerjee, R., Zhao, J., He, C., 2011. Selective fluorescent probes for live-cell monitoring of sulphide. Nat. Commun. 2, 495.

Sanchís, J., Jaén-Gil, A., Gago-Ferrero, P., Munthali, E., Farré, M., 2020. Characterization of organic matter by HRMS in surface waters: effects of chlorination on molecular fingerprints and correlation with DBP formation potential. Water Res 176 (24), 115743.

Stubbins, A., Spencer, R.G.M., Chen, H., Hatcher, P.G., Mopper, K., Hernes, P.J., Mwamba, V.L., Mangangu, A.M., Wabakanghanzi, J.N., Six, J., 2010. Illuminated darkness: molecular signatures of congo river dissolved organic matter and its photochemical alteration as revealed by ultrahigh precision mass spectrometry. Limnol. Oceanogr. 55 (4), 1467–1477.

Ulu, F., Gengec, E., Kobya, M., 2019. Removal of natural organic matter from Lake Terkos by EC process: studying on removal mechanism by floc size and zeta potential measurement and characterization by HPSEC method. J. Water Process. Eng. 31, 100831.

Wagner, E.D., Plewa, M.J., 2017. CHO cell cytotoxicity and genotoxicity analyses of disinfection by-products: an updated review. J. Environ. Sci 58, 64–76.

Walsh, M.E., Gagnon, G., Alam, Z., Andrews, R.C., 2008. Biostability and disinfectant by-product formation in drinking water blended with UF-treated filter backwash water. Water Res 42 (8–9), 2135–2145.

Wang, X., Zhang, H., Zhang, Y., Shi, Q., Wang, J., Yu, J., Yang, M., 2017. New insights into trihalomethane and haloacetic acid formation potentials: correlation with the molecular composition of natural organic matter in source water. Environ. Sci. Technol. 51 (4), 2015–2021.

Westerhoff, P., Herckes, P., Fischer, N., Donovan, S., Atkinson, A., Corwell, D., Brown, R., Croue, J.P., 2019. Linge, K. L., Liew, D., Lowe, A. Understanding the source and fate of polymer-derived nitrosamine precursors. Water Research Foundation: Denver. 174.

Yang, X., Shen, Q., Guo, W., Peng, J., Liang, Y., 2012. Precursors and nitrogen origins of trichloronitromethane and dichloroacetonitrile during chlorination/chloramination. Chemosphere 88 (1), 25–32.

Zhang, B., Shan, C., Hao, Z., Liu, J., Wu, B., Pan, B., 2019. Transformation of dissolved organic matter during full-scale treatment of integrated chemical wastewater: molecular composition correlated with spectral indexes and acute toxicity. Water Res 157, 472–482.

Zhang, L., Gu, P., Zhong, Z., Yang, D., He, W., Han, H., 2009. Characterization of organic matter and disinfection by-products in membrane backwash water from drinking water treatment. J. Hazard. Mater. 168 (2–3), 753–759.

Zhang, H., Zhang, Y., Shi, Q., Hu, J., Chu, M., Yu, J., Yang, M., 2012a. Study on transformation of natural organic matter in source water during chlorination and its chlorinated products using ultrahigh resolution mass spectrometry. Environ. Sci. Technol. 46 (8), 4396–4402.

Zhang, H., Zhang, Y., Shi, Q., Ren, S., Yu, J., Ji, F., Luo, W., Yang, M., 2012b. Characterization of low molecular weight dissolved natural organic matter along the

treatment trait of a waterworks using Fourier transform ion cyclotron resonance mass spectrometry. Water Res 46 (16), 5197–5204.
Zhang, Y., Zhang, N., Zhao, P., Niu, Z., 2018. Characteristics of molecular weight distribution of dissolved organic matter in bromide-containing water and disinfection by-product formation properties during treatment processes. J. Environ. Sci. (China) 65 (03), 179–189.
Zhao, Y., Xiao, F., Wang, D., Yan, M., Bi, Z., 2013. Disinfection byproduct precursor removal by enhanced coagulation and their distribution in chemical fractions. J. Environ. Sci. (China) 25 (11), 2207–2213.